Cover Page

Universiteit Leiden

The handle http://hdl.handle.net/1887/138855 holds various files of this Leiden University dissertation.

Author: Janssen, L.G.M.
Title: Cardiometabolic disease in South Asians: Risk factors and therapeutic strategies
Issue date: 2021-01-13

6

Twelve weeks of exenatide treatment increases [^{18}F]fluorodeoxyglucose uptake by brown adipose tissue without affecting oxidative resting energy expenditure in nondiabetic males

Laura G.M. Janssen*, Kimberly J. Nahon*, Katrien F.M. Bracké, Dennis van den Broek, Renée Smit, Aashley S.D. Sardjoe Mishre, Lisa L. Koorneef, Borja Martinez-Tellez, Jedrzej Burakiewicz, Hermien E. Kan, Floris H.P. van Velden, Lenka M. Pereira Arias-Bouda, Lioe-Fee de Geus-Oei, Jimmy F.P. Berbée, Ingrid M. Jazet, Mariëtte R. Boon*, Patrick C.N. Rensen*

*shared authorship

Metabolism 2020;106:154167

ABSTRACT

Aims/hypothesis

Brown adipose tissue (BAT) improves energy metabolism by combusting glucose and lipids into heat. Agonism of the glucagon-like peptide-1 receptor (GLP-1R) within the central nervous system activates BAT in mice. Moreover, in patients with type 2 diabetes, GLP-1R agonism lowers body weight and improves glucose and lipid levels, possibly involving BAT activation. Interestingly, people from South Asian descent are prone to develop cardiometabolic disease. We studied the effect of GLP-1R agonism on BAT in humans, specifically in South Asians and Europids without obesity or type 2 diabetes.

Methods

Twelve Dutch South Asian and 12 age- and BMI-matched Europid nondiabetic men received 12 weeks extended-release exenatide (Bydureon) in this single-arm prospective study. Before and after treatment, BAT was visualized by a cold-induced [^{18}F]FDG-PET/CT scan and a thermoneutral MRI scan, and resting energy expenditure (REE), substrate oxidation, body composition and fasting plasma glucose and serum lipids were determined. Appetite was rated using a visual analogue scale.

Results

Since the effect of exenatide on metabolic parameters did not evidently differ between ethnicities, data of all participants were pooled. Exenatide decreased body weight (-1.5 ± 0.4 kg, $p < 0.01$), without affecting REE or substrate oxidation, and transiently decreased appetite ratings during the first weeks. Exenatide also lowered triglycerides (-15%, $p < 0.05$) and total cholesterol (-5%, $p < 0.05$), and tended to lower glucose levels. Notably, exenatide increased BAT metabolic volume ($+28\%$, $p < 0.05$) and mean standardized uptake value ($+11\%$, $p < 0.05$) ([^{18}F]FDG-PET/CT), without affecting supraclavicular adipose tissue fat fraction (MRI).

Conclusions/interpretation

We show for the first time that GLP-1R agonism increases [^{18}F]FDG uptake by BAT in South Asian and Europid men without obesity or type 2 diabetes.

Trial registry: Clinicaltrials.gov NCT03002675

INTRODUCTION

Obesity has a major impact on healthcare costs, by contributing to dysregulated glucose metabolism and dyslipidaemia which may eventually culminate in type 2 diabetes and cardiovascular disease [1]. People from South Asian descent are especially prone to develop these unfavorable metabolic traits, with also higher morbidity and mortality rates compared with other ethnicities [2]. In presence of cardiometabolic disease during obesity, pharmacotherapy may be considered as an adjunct to lifestyle therapy to further enhance weight loss [3,4]. Glucagon-like peptide-1 receptor (GLP-1R) agonists have proven efficacy in the treatment of both obesity and type 2 diabetes by lowering body weight and improving glucose regulation [3–5].

Glucagon-like peptide-1 (GLP-1) is produced by the intestine upon food intake. GLP-1 subsequently lowers blood glucose levels via stimulating pancreatic insulin secretion and lowering glucagon secretion, an effect that can be mimicked by GLP-1R agonism [6]. In addition to improving postprandial glycaemia, GLP-1R agonists are well-known to induce weight loss. This weight-lowering effect of GLP-1R agonists occurs at least in part by lowering food intake via a combination of reducing appetite, increasing satiety and delaying gastric emptying [6]. Furthermore, GLP-1R agonists are associated with a modest improvement of lipid profile [7] and, albeit not consistently, an increase in resting energy expenditure (REE) in patients with type 2 diabetes [8,9]. Interestingly, preclinical evidence indicates that energy-combusting brown adipose tissue (BAT) contributes to the various beneficial metabolic effects of GLP-1R agonists [8,10,11]. More specifically, central GLP-1R agonism in mice was shown to increase plasma triglyceride-derived fatty acid and glucose uptake by BAT and to shift substrate utilization towards lipid oxidation [10,12].

In this study, we hypothesized that chronic GLP-1R agonism activates BAT in humans, thereby contributing to weight loss and improved plasma glucose and lipid levels. As a proof of concept, we investigated the effect of 12 weeks extended-release exenatide on BAT measured by [^{18}F]fluorodeoxyglucose positron emission tomography/computed tomography ([^{18}F]FDG-PET/CT) and magnetic resonance imaging (MRI) scans in South Asian and Europid men without obesity or diabetes. In addition, we evaluated the effect of exenatide on body weight and composition, energy metabolism and plasma glucose and lipid levels.

METHODS

See the supplemental material for an extensive description of all analyses.

2.1. Power calculation and participants

We regarded an increase in BAT activity assessed by [^{18}F]FDG-PET/ CT of 13% as clinically relevant, and with an SD of 13, α of 0.05 and β of 80% this resulted in 12 subjects per arm. Therefore, twelve healthy nondiabetic Dutch South Asian and 12 Dutch Europid men were included in this study. South Asians and Europids were matched for age (20–36 years) and BMI (18–27 kg/m^2). Exclusion criteria were smoking, recent participation in a weight loss or exercise program, any significant chronic disease or renal, hepatic or endocrine disease, use of medication known to influence glucose or lipid metabolism or BAT activity (e.g. beta blockers), participation in another study including a pharmaceutical drug and any contra-indications to undergo an MRI scan.

2.2. Study approval

This study was performed in accordance with the principles of the revised declaration of Helsinki [13] and approved by the medical ethical committee of the Leiden University Medical Center (LUMC). All participants provided written informed consent prior to participation.

2.3. Study design

This single-arm prospective study was conducted between September 2016 and February 2018 at the LUMC. Participants received extended-release exenatide (Bydureon, AstraZeneca B.V., The Hague, the Netherlands) 2 mg s.c. once weekly during 12 weeks. Side-effects and general wellbeing were monitored weekly. Changes in dietary habits and physical activity were discouraged. Appetite ratings were monitored every 4 weeks with a visual analogue scale (VAS), which was filled in during the day in between meals. A study day was conducted before and after exenatide treatment (**Supplemental Fig. 1**). The post-exenatide study day was performed one week after the last injection. Participants were instructed to refrain from physical exercise 48 h prior to these study days and to consume a standardized meal the evening prior to the study days. After a 10-hour overnight fast, body composition was determined by bio-impedance analysis (Bodystat 1500, Bodystat, Douglas, Isle of Man, UK) and an intravenous cannula was placed in the antecubital vein. An MRI scan (3 T MRI, Philips Ingenia, Philips Healthcare, Best, the Netherlands) was then performed at room temperature to assess the fat fraction and volume of the supraclavicular adipose tissue depot. Afterwards, wireless iButton temperature loggers were attached to 14 ISO-defined positions to measure skin temperature [14], and participants took place in a semi supine position on a bed between two water-

perfused blankets (Blanketrol® III, Cincinnati Sub-Zero Products, Inc., Cincinnati, Ohio, USA) set at a temperature of 32 °C (considered thermoneutrality) for a period of 45 min. During the final 30 min, REE was measured by indirect calorimetry (JAEGER™ Vyntus™ CPX, Carefusion, Hochberg, Germany), followed by a blood draw. Next, a personalized cooling protocol was applied as described previously [15]. Briefly, the water temperature was gradually decreased to a minimum of 9 °C during 1 h, followed by a gradual increase of 2–3 °C, which happened earlier in case of shivering. Shivering was reported by the participants and visually assessed by the researchers. Subsequently, cold-induced REE was measured, whereafter 74 MBq [^{18}F]FDG was administered intravenously and followed by a PET/CT scan after 1 h of incubation (Horizon with TrueV option, Siemens Healthcare, Knoxville, USA). The cooling protocol continued until start of the PET/CT. One South Asian participant was excluded from all [^{18}F]FDG-PET/CT analyses due to excessive movement during a scan.

2.4. Serum and plasma measurements

Commercially available enzymatic kits were used to measure serum concentrations of triglycerides, total cholesterol and HDL-cholesterol (all Roche Diagnostics, Woerden, the Netherlands), free fatty acids (Wako chemicals, Nuess, Germany) and insulin (Meso Scale Diagnostics LLC, Rockville, MD, USA), and plasma glucose (Instruchemie, Delfzijl, the Netherlands). LDL-cholesterol was calculated by the Friedewald equation [16].

2.5. Statistical analysis

Statistical analyses were performed with SPSS Statistics (version 20.0, IBM Corporation, Armonk, NY, USA) and GraphPad Prism (version 8.0.1.244, GraphPad Software, La Jolla, CA, USA). Baseline characteristics were compared between ethnicities with a two-tailed unpaired Student's t-test. Comparisons between variables measured at a similar temperature were performed with a two-factor mixed design ANOVA, as they included two factors: exenatide treatment (within-subjects) and ethnicity (between subjects). Comparisons between variables measured during both thermoneutrality and cold were analysed with linear mixed models, which included temperature, exenatide treatment and ethnicity as fixed factors, and temperature and exenatide treatment as random effects. For the random effects, i.e. random slopes and intercepts, the model used an unstructured covariance matrix. P-values are shown for main effects and interactions as well as for post hoc tests. Correlation analyses were performed using linear regression analysis and assessed for interaction of ethnicity. A p-value < 0.05 was considered statistically significant. Data are presented as mean ± SEM.

RESULTS

3.1 Participant characteristics and compliance

One participant dropped out of the study prior to the first study day and was replaced by a newly recruited participant. Twenty-four participants completed the study. Clinical characteristics are shown in **Table 1**. Blood pressure and heart rate as well as fasting total cholesterol, triglyceride and glucose levels were within a healthy range. When comparing baseline characteristics between ethnicities, South Asians were shorter than Europids (1.78 ± 0.02 *vs* 1.85 ± 0.02 m, $p < 0.01$). Age and BMI were comparable between South Asians and Europids, as they were matched for these parameters. Total cholesterol, triglyceride and glucose levels were also comparable between ethnicities.

The weekly s.c. injections with exenatide were generally well tolerated. The most frequently reported side-effects were mild and transient, and were of gastro-intestinal (e.g. nausea, vomiting) and dermatological origin (e.g. subcutaneous nodule). No serious adverse events occurred.

Table 1. Participant characteristics

	All participants (N=24)	Europids (N=12)	South Asians (N=12)
Age (yr)	26.5±0.7	25.6±0.9	27.5±0.9
Height (m)	1.82±0.01	1.85±0.02	1.78±0.02 ††
Weight (kg)	79.3±2.1	81.6±2.6	77.0±3.3
BMI (kg/m^2)	23.9±0.5	23.8±0.7	24.1±0.8
Serum total cholesterol (mmol/L)	4.6±0.2	4.5±0.2	4.8±0.2
Serum triglycerides (mmol/L)	0.98±0.07	0.96±0.10	1.00±0.11
Plasma glucose (mmol/L)	5.0±0.1	5.0±0.1	4.9±0.2
Systolic blood pressure (mmHg)	121±2	125±4	118±2
Diastolic blood pressure (mmHg)	76±2	76±3	75±2
Heart rate (bpm)	62±2	66±4	58±3 ˜

Fasted serum lipid and plasma glucose levels are shown. Data were analysed by an unpaired students t-test and presented as mean ± SEM. ˜$p < 0.1$, ††$p < 0.01$, South Asians *vs* Europids.

3.2. Exenatide lowers body weight without affecting resting energy expenditure

We firstly assessed the effect of exenatide on body weight and composition in our cohort of non-obese men (**Supplemental Table 1**). Exenatide lowered body weight in the total cohort (−1.5 ± 0.4 kg, $p < 0.01$), mainly due to a reduction in lean mass (−1.1 ± 0.4 kg, $p < 0.01$) rather than fat mass, without affecting the waist-to-hip ratio. We then evaluated whether ethnicity modifies the effect of exenatide on these parameters. Here, we

observed a trend towards interaction between the effects of ethnicity and exenatide on fat mass ($p = 0.059$), reflecting a decreased fat mass after exenatide only in South Asians (-1.0 ± 0.4 kg, $p < 0.05$) but not in Europids (0.2 ± 0.4, $p = 0.68$, **Supplemental Table 1**). Body fat percentage was higher in South Asians compared with Europids at baseline (18.9 ± 0.9 *vs* $14.5 \pm 1.4\%$, $p < 0.01$), which remained present after exenatide treatment (18.1 ± 0.8 *vs* $14.9 \pm 1.2\%$, $p < 0.05$, **Supplemental Table 1**). Of note, we observed a negative correlation between baseline body fat percentage and the exenatide-induced delta fat percentage (data not shown).

Hereafter, we investigated whether an altered energy metabolism could underlie these weight-lowering effects of exenatide. Aside from a trend towards a lower glucose oxidation, exenatide did not evidently affect the REE (nor when corrected for lean mass), respiratory quotient (RQ) or substrate oxidation in the total study cohort (**Fig. 1**) or when studying ethnicities separately (**Supplemental Fig. 2**). As expected, both before and after exenatide, cold exposure increased REE (+7%, $p < 0.01$ and + 11%, $p < 0.001$) and lowered the RQ (−5%, $p < 0.001$ and −3%, $p < 0.05$), reflected by an increased lipid oxidation (+35%, $p < 0.001$ and +28%, $p < 0.001$) and decreased glucose oxidation (−28%, $p < 0.01$ and −14%, $p = 0.12$) in the total study cohort (**Fig. 1**), which was not significantly different before and after exenatide.

We next investigated the role of a lowered appetite in the weightlowering effect of exenatide (**Fig. 2**). In the total study cohort exenatide reduced the hunger sensation (−27%, $p < 0.05$) and desire to eat (−25%, $p < 0.05$) after 4 weeks, which was transient. Furthermore, exenatide did not overtly affect the sensation of fullness or satiety. Ethnicity did not modify the effect of exenatide on these appetite ratings (**Supplemental Fig. 3**).

3.3. Exenatide lowers serum lipid levels and tends to lower plasma glucose levels

We next evaluated the effect of exenatide on glucose and lipid levels (**Fig. 3**). In the total study cohort, the main treatment effect showed that exenatide lowered triglycerides (−15%, $p < 0.05$), without affecting free fatty acids. In addition, exenatide lowered total cholesterol (−5%, $p < 0.05$), which was attributable to a trend towards a lowering of LDLcholesterol (−5%, $p = 0.10$) probably in addition to lowering of VLDL/ remnant-cholesterol, rather than HDL-cholesterol. Lastly, exenatide tended to lower plasma glucose (4.6 ± 0.1 *vs* 4.7 ± 0.0 mmol/L, $p = 0.09$) without affecting serum insulin levels. Ethnicity did not modify these effects of exenatide on lipid and glucose levels (**Supplemental Fig. 4**). However, when comparing ethnicities at baseline (**Supplemental Fig. 4**), total cholesterol tended to be higher in South Asians compared with Europids (4.8 ± 0.2 *vs* 4.2 ± 0.1 mmol/L, $p = 0.05$), explained by a trend towards higher LDL-cholesterol in South Asians compared with Europids (3.3 ± 0.3 *vs* 2.7 ± 0.1 mmol/L, $p = 0.07$). Furthermore,

plasma glucose tended to be higher in South Asians compared with Europids at baseline (4.8 ± 0.1 *vs* 4.6 ± 0.1 mmol/L, p = 0.08).

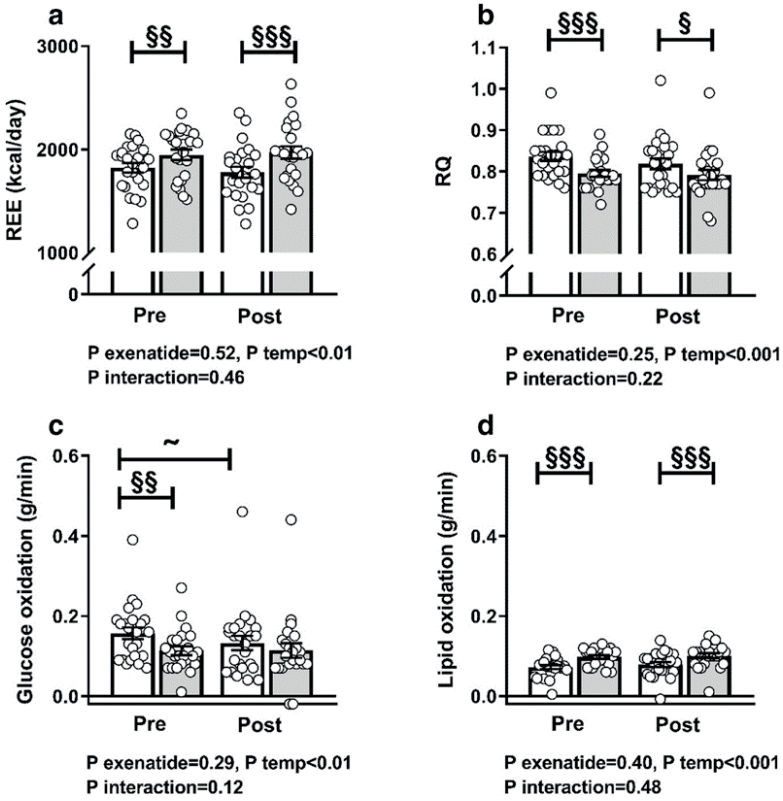

Fig. 1. Exenatide does not affect energy metabolism.
The effect of exenatide on thermoneutral and cold-induced resting energy expenditure (REE) (a), respiratory quotient (RQ) (b), glucose oxidation (c) and lipid oxidation (d) in the total study cohort (N = 24). Pre = before exenatide, post = after exenatide. Data were analysed by linear mixed models and are presented as mean ± SEM. White bars are thermoneutral, grey bars are during short term cooling. p-Values for the main effect of exenatide treatment (exenatide) and temperature (temp) and their interaction (exenatide*temp) are shown below the figures. ˜p < 0.1 post-hoc p-value post vs pre exenatide. §p < 0.05, §§p < 0.05, §§§p < 0.001 post-hoc p-values cold vs thermoneutrality.

3.4. Exenatide decreases the systolic blood pressure and increases the heart rate

As GLP-1R agonists are known to affect the cardiovascular system [17], we evaluated the effect of exenatide on blood pressure and heart rate in our study (**Supplemental Table 2**). In the total study cohort, exenatide lowered the systolic blood pressure (–4 ± 1 mm Hg, p < 0.01) without affecting the diastolic blood pressure, and increased the heart rate (+6 ± 1 bpm, p < 0.001). When assessing whether ethnicity modifies the effect

of exenatide on these outcome parameters, we observed that the increase in heart rate was more pronounced in South Asians compared with Europids (+8 ± 1 *vs* +3 ± 1 bpm, p < 0.05; **Supplemental Table 2**).

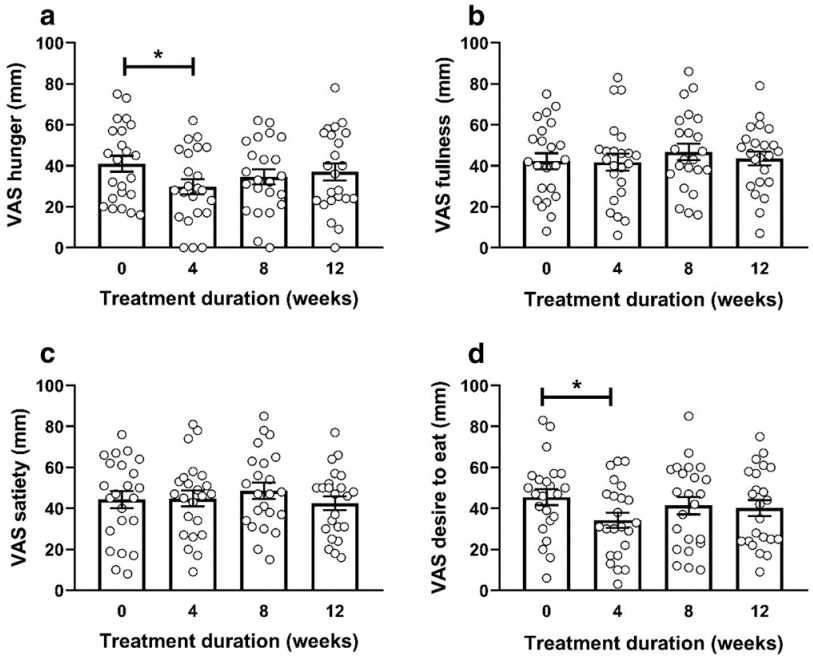

Fig. 2. Exenatide lowers the sensation of hunger and desire to eat during the first weeks of treatment. The effect of exenatide on subjective ratings for hunger (a), fullness (b), satiety (c) and desire to eat (d) measured every 4 weeks in the total study cohort (N = 23). One of the 12 South Asian participants was excluded due to incomplete questionnaires. Higher values (mm) indicate higher ratings. Data were analysed by a two factor mixed design ANOVA and are presented as mean ± SEM. *p < 0.05 effect of exenatide.

3.5. Exenatide enhances [^{18}F]FDG uptake by brown adipose tissue

We next studied the effect of exenatide on BAT [^{18}F]FDG uptake (**Fig. 4**). Notably, in the total study cohort exenatide increased the metabolic volume (+28%, p < 0.05) and mean standardized uptake value (SUVmean) (+11%, p < 0.05) of classical BAT regions, i.e. cervical and supraclavicular depots. Similar results were observed when additionally including the upper mediastinal, axillary and paravertebral BAT depots (**Supplemental Table 3**). Of note, the effect of exenatide on BAT parameters could not be explained by seasonal variation or by changes in body weight or composition (data not shown). The mean water temperature to which participants were exposed during the personalized cooling protocol was also comparable after exenatide (data not shown). Ethnicity did not interact with the effect of exenatide on BAT parameters, and BAT parameters

were comparable between South Asians and Europids at baseline (**Supplemental Table 3**). Moreover, exenatide did not affect the [^{18}F]FDG uptake of the subcutaneous or visceral white adipose tissue depots (**Supplemental Table 4**). Exenatide did increase

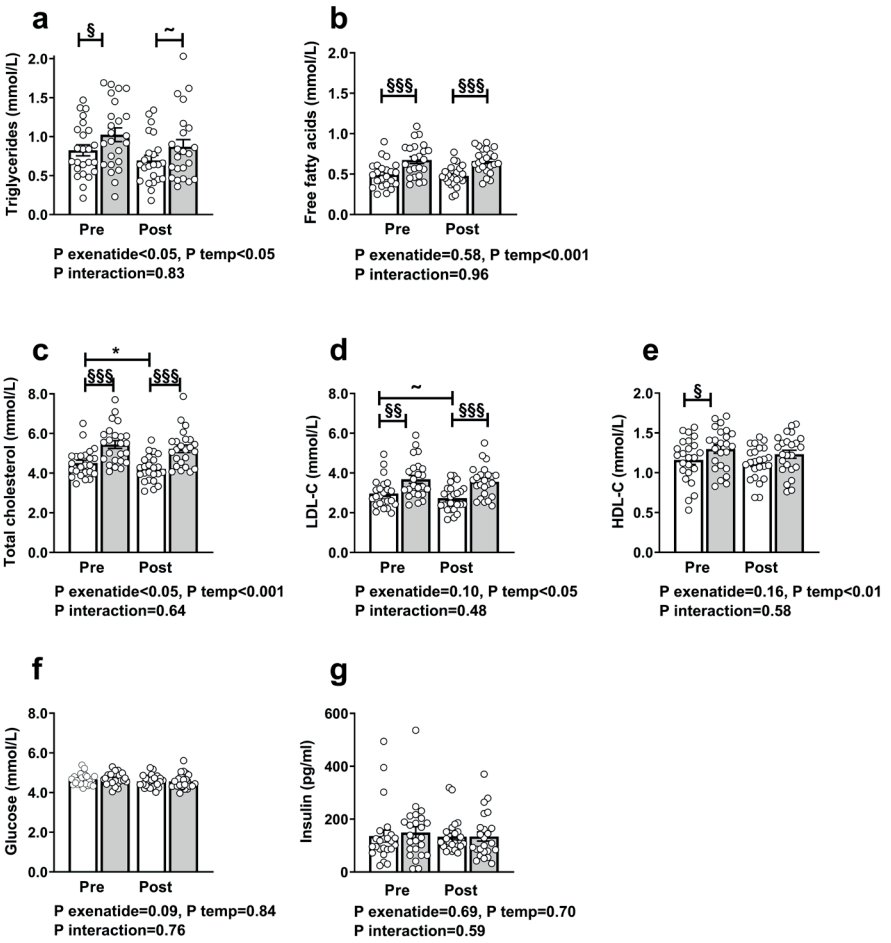

Fig. 3. Exenatide lowers total triglyceride and cholesterol levels, and tends to lower plasma glucose levels. The effect of exenatide on thermoneutral and cold-induced fasted serum triglycerides (a), free fatty acids (b), total cholesterol (c), LDL-cholesterol (LDL-C) (d), HDL-cholesterol (HDL-C) (e), plasma glucose (f) and serum insulin (g) levels in the total study cohort (N = 24). Pre = before exenatide, post = after exenatide. Data were analysed by linear mixed models and are presented as mean ± SEM. White bars are thermoneutral, grey bars are during short term cooling. P-values for the main effect of exenatide treatment (exenatide) and temperature (temp) and their interaction (exenatide*temp) are shown below the figures. ˜p < 0.1, *p < 0.05 post-hoc p-values post vs pre exenatide. ˜p < 0.1, §p < 0.05, §§p < 0.01, §§§p < 0.001 post-hoc p-values cold *vs* thermoneutrality

the SUVmean of the pectoralis major muscle (+16%, $p < 0.05$) and psoas major muscle (+27% g/mL, $p < 0.001$) and decreased the SUVmean of the trapezius muscle (−15%, $p < 0.05$) (**Supplemental Table 4**). Ethnicity affected the exenatide-induced decrease in SUVmean of the trapezius muscle ($p < 0.05$ for interaction), reflecting a significant decrease in SUVmean of the trapezius muscle only in South Asians (−24%, $p < 0.01$) but not in Europids (−4%, $p = 0.72$) (**Supplemental Table 4**).

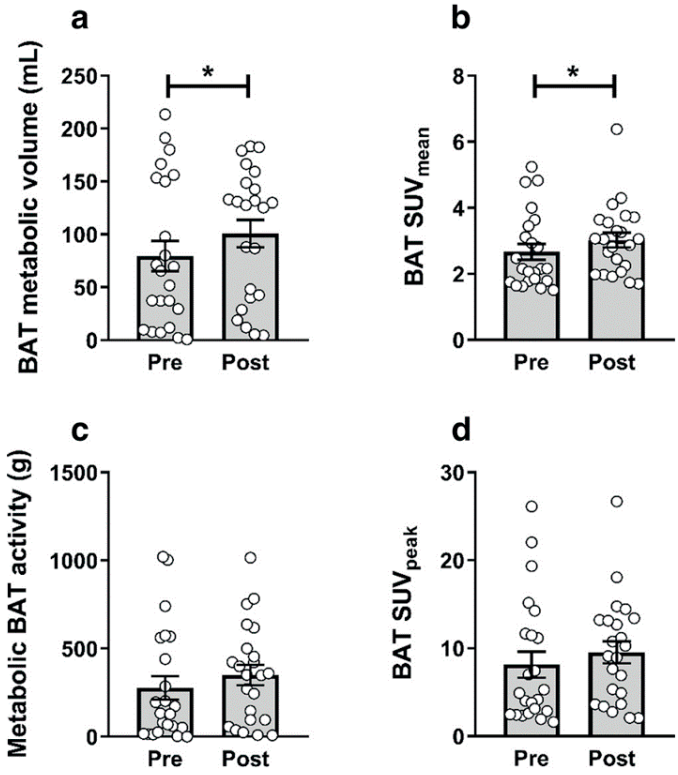

Fig. 4. Exenatide increases brown adipose tissue metabolic volume and SUVmean.
The effect of exenatide on metabolic volume (a), mean standardized uptake value (SUVmean) (b), metabolic activity (c) and peak standardized uptake value (SUVpeak) (d) of classical brown adipose tissue (BAT) depots in the total study cohort (N = 23). One of the 12 South Asian participants was excluded due to movement during a scan. Pre = before exenatide, post = after exenatide. Data were analysed by a two factor mixed design ANOVA and are presented as mean ± SEM. *$p < 0.05$ post vs pre exenatide.

3.6. Exenatide does not affect supraclavicular adipose tissue fat fraction measured with MRI

Lastly, as BAT activation lowers the fat fraction of classical BAT depots by combusting intracellular triglycerides [18], we evaluated the effect of exenatide on supraclavicular

adipose tissue by MRI. Both the fat fraction (post 0.745 ± 0.008 *vs* pre 0.745 ± 0.009, p = 0.96) and volume (post 30.2 ± 2.9 *vs* pre 31.0 ± 2.8 mL, p = 0.22) of this adipose tissue depot remained unaltered after exenatide in the total study cohort (**Fig. 5**) or in either ethnicity (**Supplemental Table 5**). Interestingly, albeit exenatide did not affect supraclavicular adipose tissue mean fat fraction or volume, Δfat fraction negatively correlated with ΔSUVmean (**Fig. 6**) and ΔSUVpeak (data not shown) on [^{18}F]FDG-PET/CT scan. Ethnicity did not affect these correlation analyses.

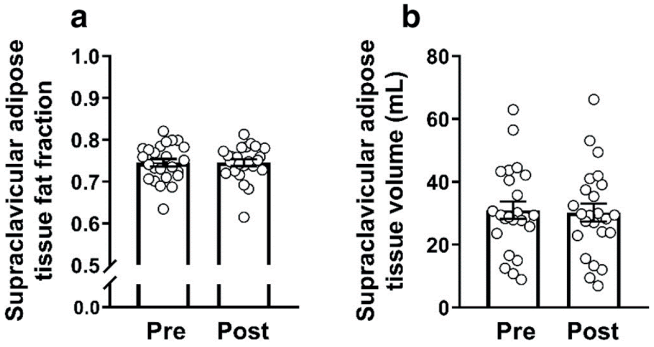

Fig. 5. Exenatide does not affect the supraclavicular adipose tissue depot fat fraction or volume.
The effect of exenatide on the supraclavicular adipose tissue depot fat fraction (a) and volume (b) in the total study cohort (N = 24). Fat fraction thresholds were set at 0.5–1.0. Pre = before exenatide, post = after exenatide. Data were analysed by a two factor mixed design ANOVA and are presented as mean ± SEM.

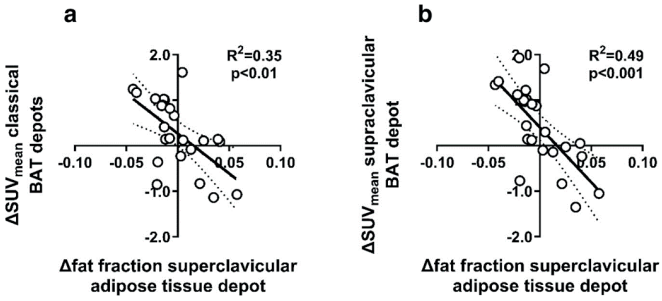

Fig. 6. Exenatide-induced changes in supraclavicular adipose tissue fat fraction (MRI) and SUVmean ([18F] FDG-PET/CT) negatively correlate.
Correlation analyses between the Δfat fraction (MRI) and ΔSUVmean ([18F]FDG-PET/CT) upon exenatide treatment of classical BAT depots (a) and only the unilateral left supraclavicular BAT depot (b). MRI fat fraction thresholds were set at 0.5–1.0. Data were analysed with linear regression analysis and assessed for interaction of ethnicity, and are presented as mean ± SEM. Dotted lines represent 95% CI.

DISCUSSION

GLP-1R agonists have multiple favorable metabolic effects additional to improving glycaemia, including weight loss and lowering lipid levels. Since preclinical studies have shown a role for central agonism of the GLP-1R in activating energy-combusting BAT, we aimed to investigate in a proof-of-principle study the effect of GLP-1R agonism on BAT metabolism in non-obese nondiabetic men. We included both South Asian and Europid participants, as we have previously shown that South Asians have an unfavorable energy metabolism compared with Europids [15]. Here, we show that exenatide lowered body weight and serum lipids already in healthy young men, without affecting REE or substrate utilization. Intriguingly, exenatide increased [^{18}F]FDG uptake by BAT, suggesting more metabolically active BAT. The metabolic effects of exenatide were largely comparable between ethnicities. Our findings support a role for the GLP-1R in BAT activation in South Asian and Europid men.

Exenatide lowered body weight in this cohort of lean to mildly overweight men. This reduction in body weight was mainly attributable to a loss of lean mass in both ethnicities, with an additional loss of fat mass in South Asian participants, without significantly affecting overall body fat percentage. The reduction in body weight in this study is in line with a meta-analysis investigating randomized controlled trials conducted in normoglycemic severe overweight or obese participants, showing a body weight reduction of 2.5–5.1 kg after 12–24 weeks of treatment with short-acting exenatide [19]. There were however only two trials included in this meta-analysis that reported body fat measurements, and these showed no significant change in overall fat mass [20] or percentage [21] compared with placebo. In concordance with previous studies [15,22], we observed a higher body fat percentage in South Asians compared with Europids. Since exercise may preserve lean mass during weight loss [23], we cannot exclude that reduced physical activity to any extent during the 12-week exenatide treatment period might have contributed to the loss of lean mass observed in our cohort of healthy young men, albeit we encouraged participants not to alter their lifestyle. We observed a negative correlation between baseline fat percentage and the delta fat percentage upon exenatide treatment, which is in line with evidence showing that higher baseline adiposity is associated with a lower relative contribution of lean mass to weight loss [24]. We therefore propose that the higher baseline body fat percentage in South Asians compared with Europids underlies their loss of fat mass after exenatide treatment.

Food intake is another major determinant of energy balance. Activation of the GLP-1R has an anorexigenic effect that contributes to weight loss [25,26]. Here, exenatide treatment did not affect overall appetite as measured by VAS. However, the sensation of hunger and desire to eat were lower during the first 4 weeks of treatment. This fits with recent studies showing that GLP-1R agonists cause changes in central nervous system

activation to food cues resulting in less reward to food [26]. These effects are temporarily, which might explain the plateau that is often reached with respect to weight loss. A study using short-term liraglutide suggests that this might be due to a decrease in fasting leptin levels, resulting in increased reward thereby counteracting the beneficial effects of liraglutide [27]. Albeit that in our study these appetite changes were transient and restored within a few weeks, a temporarily reduced food intake presumably contributed to the weight loss of some participants. Interestingly, however, preclinical evidence showed that weight loss was less pronounced in mice that were pair-fed to mice treated with centrally administrated exendin-4 [10]. Moreover, in mice treated chronically with peripherally administered exendin-4, weight loss continued even after food intake was restored within a few weeks after initiation of treatment [28]. These murine studies thus suggest that the weight-lowering effect of GLP-1R agonism goes beyond merely reducing food intake.

To investigate whether GLP-1R agonism induces weight loss in part by stimulating energy combustion, we evaluated the effect of exenatide on REE and substrate utilization. In our study, exenatide did not affect REE in the total study cohort or in either ethnicity. So far, only two clinical trials have reported an effect of exenatide on REE; one study investigating short-term treatment with liraglutide in patients with type 2 diabetes [9], and one study investigating long-term treatment with either liraglutide or exenatide in patients with type 2 diabetes [8]. However, our results are in agreement with most studies investigating the effect of prolonged (5–16 weeks) treatment with a GLP-1R agonist on energy metabolism, which did not observe differences in REE or any of the other components of total energy expenditure (i.e. the thermic effects of feeding and physical activity) [21,29–31]. We cannot exclude that a possible increase in REE by exenatide is masked in our study by a lowering in REE that generally accompanies weight loss [32]. Exenatide did also not affect substrate utilization in our study. This observation is in concordance with Beiroa et al. [8], who showed an unchanged substrate utilization in patients with type 2 diabetes after one year of treatment with either exenatide or liraglutide on top of metformin. On the contrary, another study showed that 4 weeks liraglutide in nondiabetic obese subjects shifted substrate oxidation from glucose towards lipids [31]. This is in line with preclinical studies showing that centrally administered GLP-1 [12] or exendin-4 [10] increased lipid oxidation in diet-induced obese mice. Possibly, the use of different variants of exenatide (long-acting vs short-acting) and the time after administration affects measures of energy balance. We can also not exclude that a shift in substrate utilization might be too subtle to detect via indirect calorimetry, especially in our study involving non-obese normoglycemic humans.

Exenatide tended to lower plasma glucose levels in our study, which may be mediated by enhanced insulin secretion due to GLP-1R agonism in pancreatic beta cells, and possibly increased peripheral insulin sensitivity [5]. Intriguingly, exenatide reduced

serum triglycerides and total cholesterol, and tended to lower LDL-cholesterol already in these normolipidemic participants. We can only speculate about the underlying mechanisms contributing to the lipid-lowering effects of exenatide. Firstly, impaired secretion of triglyceride-rich lipoproteins into the circulation (i.e. VLDL from the liver and chylomicrons from the small intestines) following GLP-1R agonism may have lowered lipid levels. In line with this, one to four weeks peripherally administered exendin-4 lowered circulating VLDL-triglyceride levels in mice, accompanied by reduced hepatic VLDL particle production. This resulted, together with decreased hepatic lipogenesis, even in reversal of high-fat diet-induced hepatic steatosis [33,34]. Likewise, an acute infusion with exenatide reduced postprandial triglyceride excursions and intestinal lipoprotein production in both healthy [35] and insulin-resistant humans [36]. On the other hand, we hypothesize that exenatide may increase lipids and glucose clearance by peripheral metabolic tissues, as we have previously shown that central administration of exendin-4 increased lipid and glucose uptake by skeletal muscle and BAT in mice [10].

To further investigate the contribution of peripheral metabolic tissues to the beneficial effects of exenatide, especially that of energycombusting BAT, we performed a cold-induced [^{18}F]FDG-PET/CT scan. This is the current gold standard to assess BAT metabolic volume and activity and involves quantifying glucose uptake by several BAT depots [37]. Here, we show for the first time that GLP-1R agonism increased BAT volume and SUVmean in humans. This is fully compatible with our previous observation that exendin-4 enhances glucose uptake by BAT in both lean and diet-induced obese mice [10], although the contribution of BAT to whole-body metabolism in rodents is more pronounced compared to humans [38]. Exenatide did not increase [^{18}F]FDG uptake by either subcutaneous or visceral white adipose tissue in the current study, suggesting that GLP-1R agonism in humans might be more involved in promoting substrate utilization by classical BAT depots rather than browning of white adipose tissue. Glucose uptake as measured by [^{18}F]FDG PET/CT scan is influenced by insulin sensitivity of the tissue [39]. Therefore, this method may underestimate measures of BAT metabolism in older subjects and/or subjects with type 2 diabetes, circumstances in which BAT becomes more insulin resistant. In our study, it could be argued that exenatide treatment increases whole-body insulin sensitivity, which would enhance glucose uptake by BAT. However, we did not observe a consistent increase in [^{18}F]FDG uptake by skeletal muscles after exenatide, supporting that the enhanced glucose uptake by BAT truly represents expansion of BAT volume. In addition, to exclude an acute effect of exenatide on BAT metabolism, the postexenatide study day was performed one week after the last injection. It would be interesting to assess whether other GLP-1R agonists, for instance liraglutide 3.0 mg that is currently approved for the treatment of obesity [40], also enhances glucose uptake specifically by BAT using [^{18}F]FDG-PET/CT. Importantly, centrally administering either exendin4 [10] or liraglutide [8] was shown to enhance sympathetic

outflow to BAT in mice. We therefore propose that increased sympathetic output may mediate the enhanced BAT volume and [^{18}F]FDG uptake during GLP-1R agonism in our human study. The increased heart rate we observed after exenatide in this study is in line with previous research [41] and may also reflect this increased sympathetic outflow.

Profound BAT activation, e.g. via applying a potent sympathetic stimulus by cooling humans until shivering, has been shown to burn intracellular lipids and thereby decrease the fat fraction of classical BAT depots [18]. However, the fat fraction and volume of the supraclavicular adipose tissue depot as measured by MRI remained unchanged after exenatide. As lipid uptake and utilization by activated BAT are strictly regulated, we cannot exclude that MRI might be unable to quantify a net increase in intracellular lipid combustion after exenatide. Although MRI is used less often to assess BAT volume compared with the [^{18}F]FDG PET/scan, a recent study showed that these two methods correlate well ($R^2 = 0.52$) in healthy adult subjects [42]. Interestingly, despite an unchanged overall supraclavicular adipose tissue fat fraction after exenatide, the Δfat fraction on MRI negatively correlated with the Δ[^{18}F]FDG uptake on PET/CT. This suggests that BAT metabolism of some participants was more sensitive to GLP-1R agonism ('responders') than that of others ('non-responders'), with a lower fat fraction being associated with more [^{18}F]FDG uptake and vice versa. Since GLP-1R agonism in mice increased the uptake of triglyceride-derived fatty acids by BAT much more robustly compared with deoxyglucose [10], it would be highly interesting to investigate whether GLP-1R agonism in humans also increases BAT fatty acid uptake and oxidative metabolism, using [^{18}F]fluorothiaheptadecanoic acid and [^{11}C]acetate tracers by PET/CT, respectively [43]. However, in this respect it should be noted that BAT in rodents has a larger contribution to resting energy expenditure as compared to BAT in humans. The precise contribution of activated human BAT to resting energy expenditure remains unclear so far but estimations based on static and dynamic [^{18}F]FDG PET/CT scans vary between 115 and 256 kcal/day [44,45]. Furthermore, we can only speculate about the contribution of increased BAT activity to the metabolic improvements observed after exenatide in this human study.

This study is not without limitations. As this study was designed without a placebo arm, we cannot exclude that intra-individual variations in energy metabolism that may occur over time have affected our results. Reassuringly, including seasonality as a covariate did not influence the statistical analyses. Furthermore, despite increased [^{18}F]FDG uptake by BAT, with our experimental set-up no effect of exenatide on resting energy expenditure was found. The absence of effect may be inherent to indirect calorimetry that we used to estimate energy expenditure, which only measures oxygen-dependent energy metabolism, and/or relate to the error of the measurement of indirect calorimetry. The increase in resting energy expenditure in humans that is expected from enhanced BAT activity is in fact modest (115 to 256 kcal/day), which may be below

the threshold of a detectable increase in energy expenditure. Notably, we previously showed by pair-feeding experiments in mice that exendin-4 reduces body fat mass despite equal food intake. Although these data by definition imply that exendin-4 increases energy expenditure in mice, increased energy expenditure was not apparent from indirect calorimetry [10]. Future studies investigating the effects of long-term BAT activation on resting energy expenditure and its metabolic consequences are therefore highly warranted, probably with more accurate and/or more advanced techniques. For future studies, we propose to include continuous measurements by means of a room calorimeter system, and employ techniques to assess the contribution of non-oxidative energy expenditure. In addition, as mentioned above, to further explore the effect of GLP-1R agonism on BAT metabolism and energy expenditure, we propose to conduct a future study with the GLP-1R agonist liraglutide 3.0 mg, that is especially potent with respect to inducing weight loss [46].

In summary, we show that prolonged GLP-1R agonism activates BAT and improves the metabolic phenotype, including serum lipid profile, already in non-obese normoglycemic young men, with largely similar effects observed in South Asian and Europid individuals. Further research investigating the effect of GLP-1R agonism on thermogenesis and substrate utilization by BAT, and the contribution of BAT to an improved cardiometabolic phenotype upon GLP-1R agonism in patients with type 2 diabetes is warranted.

FUNDING

This research was conducted with support from AstraZeneca BV. This study was also supported by the Dutch Diabetes Research Foundation (Junior Postdoc Fellowship; 2015.81.1808 to MRB) and the Netherlands CardioVascular Research Initiative; an initiative with support of the Dutch Heart Foundation (CVON2017-20 GENIUS-II to PCNR).

ACKNOWLEDGEMENTS

Glucose monitors and test strips were kindly provided by Roche Diabetes Care Nederland BV (Almere, the Netherlands). We thank Trea Streefland (Dept. of Medicine, Div. of Endocrinology, LUMC), Jordi Vonk-van Oosten and Inge Enthoven (both Dept. of Radiology, C.J. Gorter Center for High Field MRI, LUMC), and Patrick van der Zwet and Petra Dibbets-Schneider (both Dept. of Radiology, Div. of Nuclear Medicine, LUMC) for their excellent technical assistance. Parts of the data in this manuscript were presented at the International Conference of Endocrinology in December 2018.

REFERENCES

1. https://www.who.int/news-room/fact-sheets/detail/obesity-and-overweight.
2. Volgman AS, Palaniappan LS, Aggarwal NT, Gupta M, Khandelwal A, Krishnan AV, et al. Atherosclerotic cardiovascular disease in South Asians in the United States: epidemiology, risk factors, and treatments: a scientific statement from the American Heart Association. Circulation 2018;138:e1-34.
3. Garvey WT, Mechanick JI, Brett EM, Garber AJ, Hurley DL, Jastreboff AM, et al. American association of clinical endocrinologists and American college of endocrinology comprehensive clinical practice guidelines for medical care of patients with obesity executive summary complete guidelines available at https://www.aace.com/publications/guidelines. Endocr Pract 2016;22:842–84.
4. Apovian CM, Aronne LJ, Bessesen DH, McDonnell ME, Murad MH, Pagotto U, et al. Pharmacological management of obesity: an endocrine society clinical practice guideline. J Clin Endocrinol Metab 2015;100:342–62.
5. Drucker DJ, Habener JF, Holst JJ. Discovery, characterization, and clinical development of the glucagon-like peptides. J Clin Invest 2017;127:4217–27.
6. Drucker DJ. Mechanisms of action and therapeutic application of glucagon-like peptide-1. Cell Metab 2018;27:740–56.
7. Sun F, Wu S, Wang J, Guo S, Chai S, Yang Z, et al. Effect of glucagon-like peptide-1 receptor agonists on lipid profiles among type 2 diabetes: a systematic review and network meta-analysis. Clin Ther 2015;37(e8):225–41.
8. Beiroa D, Imbernon M, Gallego R, Senra A, Herranz D, Villarroya F, et al. GLP-1 agonism stimulates brown adipose tissue thermogenesis and browning through hypothalamic AMPK. Diabetes 2014;63:3346–58.
9. Horowitz M, Flint A, Jones KL, Hindsberger C, Rasmussen MF, Kapitza C, et al. Effect of the once-daily human GLP-1 analogue liraglutide on appetite, energy intake, energy expenditure and gastric emptying in type 2 diabetes. Diabetes Res Clin Pract 2012;97:258–66.
10. Kooijman S, Wang Y, Parlevliet ET, Boon MR, Edelschaap D, Snaterse G, et al. Central GLP-1 receptor signalling accelerates plasma clearance of triacylglycerol and glucose by activating brown adipose tissue in mice. Diabetologia 2015;58:2637–46.
11. Lockie SH, Heppner KM, Chaudhary N, Chabenne JR, Morgan DA, Veyrat-Durebex C, et al. Direct control of brown adipose tissue thermogenesis by central nervous system glucagon-like peptide-1 receptor signaling. Diabetes 2012;61:2753–62.
12. Nogueiras R, Perez-Tilve D, Veyrat-Durebex C, Morgan DA, Varela L, Haynes WG, et al. Direct control of peripheral lipid deposition by CNS GLP-1 receptor signaling is mediated by the sympathetic nervous system and blunted in diet-induced obesity. J Neurosci 2009;29:5916–25.
13. General Assembly of the World Medical A. World Medical Association Declaration of Helsinki: ethical principles for medical research involving human subjects. J Am Coll Dent 2014;81:14–8.
14. van Marken Lichtenbelt WD, Daanen HA, Wouters L, Fronczek R, Raymann RJ, Severens NM, et al. Evaluation of wireless determination of skin temperature using iButtons. Physiol Behav 2006;88:489–97.
15. Bakker LE, Boon MR, van der Linden RA, Arias-Bouda LP, van Klinken JB, Smit F, et al. Brown adipose tissue volume in healthy lean south Asian adults compared with white Caucasians: a prospective, case-controlled observational study. Lancet Diabetes Endocrinol 2014;2:210–7.
16. Friedewald WT, Levy RI, Fredrickson DS. Estimation of the concentration of low-density lipoprotein cholesterol in plasma, without use of the preparative ultracentrifuge. Clin Chem 1972;18:499–502.

17. Monami M, Dicembrini I, Nardini C, Fiordelli I, Mannucci E. Effects of glucagon-like peptide-1 receptor agonists on cardiovascular risk: a meta-analysis of randomized clinical trials. Diabetes Obes Metab 2014;16:38–47.
18. Stahl V, Maier F, Freitag MT, Floca RO, Berger MC, Umathum R, et al. In vivo assessment of cold stimulation effects on the fat fraction of brown adipose tissue using DIXON MRI. J Magn Reson Imaging 2017;45:369–80.
19. Su N, Li Y, Xu T, Li L, Kwong JS, Du H, et al. Exenatide in obese or overweight patients without diabetes: a systematic review and meta-analyses of randomized controlled trials. Int J Cardiol 2016;219:293–300.
20. Kelly AS, Rudser KD, Nathan BM, Fox CK, Metzig AM, Coombes BJ, et al. The effect of glucagon-like peptide-1 receptor agonist therapy on body mass index in adolescents with severe obesity: a randomized, placebo-controlled, clinical trial. JAMA Pediatr 2013;167:355–60.
21. Dushay J, Gao C, Gopalakrishnan GS, Crawley M, Mitten EK, Wilker E, et al. Shortterm exenatide treatment leads to significant weight loss in a subset of obese women without diabetes. Diabetes Care 2012;35:4–11.
22. Shah AD, Kandula NR, Lin F, Allison MA, Carr J, Herrington D, et al. Less favorable body composition and adipokines in South Asians compared with other US ethnic groups: results from the MASALA and MESA studies. Int J Obes (Lond) 2016;40:639–45.
23. Heymsfield SB, Thomas D, Nguyen AM, Peng JZ, Martin C, Shen W, et al. Voluntary weight loss: systematic review of early phase body composition changes. Obes Rev 2011;12:e348–61.
24. Forbes GB. Lean body mass-body fat interrelationships in humans. Nutr Rev 1987; 45:225–31
25. van Bloemendaal L, Ten Kulve JS, la Fleur SE, Ijzerman RG, Diamant M. Effects of glucagon-like peptide 1 on appetite and body weight: focus on the CNS. J Endocrinol 2014;221:T1–16.
26. van Bloemendaal L, RG IJ, Ten Kulve JS, Barkhof F, Konrad RJ, Drent ML, et al. GLP-1 receptor activation modulates appetite- and reward-related brain areas in humans. Diabetes 2014;63:4186–96.
27. Farr OM, Tsoukas MA, Triantafyllou G, Dincer F, Filippaios A, Ko BJ, et al. Short-term administration of the GLP-1 analog liraglutide decreases circulating leptin and increases GIP levels and these changes are associated with alterations in CNS responses to food cues: a randomized, placebo-controlled, crossover study. Metabolism 2016;65:945–53.
28. Xu F, Lin B, Zheng X, Chen Z, Cao H, Xu H, et al. GLP-1 receptor agonist promotes brown remodelling in mouse white adipose tissue through SIRT1. Diabetologia 2016;59:1059–69.
29. Bradley DP, Kulstad R, Racine N, Shenker Y, Meredith M, Schoeller DA. Alterations in energy balance following exenatide administration. Appl Physiol Nutr Metab 2012; 37:893–9.
30. Harder H, Nielsen L, Tu DT, Astrup A. The effect of liraglutide, a long-acting glucagonlike peptide 1 derivative, on glycemic control, body composition, and 24-h energy expenditure in patients with type 2 diabetes. Diabetes Care 2004;27:1915–21.
31. van Can J, Sloth B, Jensen CB, Flint A, Blaak EE, Saris WH. Effects of the once-daily GLP-1 analog liraglutide on gastric emptying, glycemic parameters, appetite and energy metabolism in obese, non-diabetic adults. Int J Obes (Lond) 2014;38:784–93.
32. Ravussin E, Burnand B, Schutz Y, Jequier E. Energy expenditure before and during energy restriction in obese patients. Am J Clin Nutr 1985;41:753–9.
33. Taher J, Baker CL, Cuizon C, Masoudpour H, Zhang R, Farr S, et al. GLP-1 receptor agonism ameliorates hepatic VLDL overproduction and de novo lipogenesis in insulin resistance. Mol Metab 2014;3:823–33.

34. Parlevliet ET, Wang Y, Geerling JJ, Schroder-Van der Elst JP, Picha K, O'Neil K, et al. GLP-1 receptor activation inhibits VLDL production and reverses hepatic steatosis by decreasing hepatic lipogenesis in high-fat-fed APOE*3-Leiden mice. PLoS One 2012;7:e49152.
35. Xiao C, Bandsma RH, Dash S, Szeto L, Lewis GF. Exenatide, a glucagon-like peptide-1 receptor agonist, acutely inhibits intestinal lipoprotein production in healthy humans. Arterioscler Thromb Vasc Biol 2012;32:1513–9.
36. Schwartz EA, Koska J, Mullin MP, Syoufi I, Schwenke DC, Reaven PD. Exenatide suppresses postprandial elevations in lipids and lipoproteins in individuals with impaired glucose tolerance and recent onset type 2 diabetes mellitus. Atherosclerosis 2010;212:217–22.
37. Chen KY, Cypess AM, Laughlin MR, Haft CR, Hu HH, Bredella MA, et al. Brown adipose reporting criteria in imaging STudies (BARCIST 1.0): recommendations for standardized FDG-PET/CT experiments in humans. Cell Metab 2016;24:210–22.
38. Carpentier AC, Blondin DP, Virtanen KA, Richard D, Haman F, Turcotte EE. Brown adipose tissue energy metabolism in humans. Front Endocrinol (Lausanne) 2018;9: 447.
39. Schilperoort M, Hoeke G, Kooijman S, Rensen PC. Relevance of lipid metabolism for brown fat visualization and quantification. Curr Opin Lipidol 2016;27:242–8.
40. Pi-Sunyer X, Astrup A, Fujioka K, Greenway F, Halpern A, Krempf M, et al. A randomized, controlled trial of 3.0 mg of liraglutide in weight management. N Engl J Med 2015;373:11–22.
41. Smits MM, Muskiet MH, Tonneijck L, Hoekstra T, Kramer MH, Diamant M, et al. Exenatide acutely increases heart rate in parallel with augmented sympathetic nervous system activation in healthy overweight males. Br J Clin Pharmacol 2016;81: 613–20.
42. Andersson J, Lundstrom E, Engstrom M, Lubberink M, Ahlstrom H, Kullberg J. Estimating the cold-induced brown adipose tissue glucose uptake rate measured by (18)F-FDG PET using infrared thermography and water-fat separated MRI. Sci Rep 2019;9:12358.
43. Blondin DP, Labbe SM, Noll C, Kunach M, Phoenix S, Guerin B, et al. Selective impairment of glucose but not fatty acid or oxidative metabolism in brown adipose tissue of subjects with type 2 diabetes. Diabetes 2015;64:2388–97.
44. Leitner BP, Huang S, Brychta RJ, Duckworth CJ, Baskin AS, McGehee S, et al. Mapping of human brown adipose tissue in lean and obese young men. Proc Natl Acad Sci U S A 2017;114:8649–54.
45. van der Lans AA, Hoeks J, Brans B, Vijgen GH, Visser MG, Vosselman MJ, et al. Cold acclimation recruits human brown fat and increases nonshivering thermogenesis. J Clin Invest 2013;123:3395–403.
46. Mehta A, Marso SP, Neeland IJ. Liraglutide for weight management: a critical review of the evidence. Obes Sci Pract 2017;3:3–14.

SUPPLEMENTAL APPENDIX

METHODS

Indirect calorimetry analysis

Carbon dioxide production (VCO_2) and oxygen consumption (VO_2) were determined per minute. VCO_2 and VO_2 were used to calculate the resting energy expenditure, respiratory quotient (RQ) and glucose and lipid oxidation as described previously [1]. Formulas were adjusted for the estimated male urinary nitrogen excretion rate. Formulas for substrate oxidation rates were as follows:

Glucose oxidation (g/min) = (4.57 VCO_2) - (3.23 * VO_2) - 0.0274456*
*Lipid oxidation (g/min) = (1.69 * VO_2) - (1.69 * VCO_2) - 0.02142868*

[^{18}F]fluorodeoxyglucose positron emission tomography/computed tomography data acquisition and analysis

The scanning protocol started with a low dose CT-scan (30 mAeff, 120kV), followed by a PET scan (ten bed positions, each lasting 5.5 minutes, from the top of the head until the iliac crest) in accordance with European Nuclear Medicine guidelines [2]. Positron emission tomography (PET) and computed tomography (CT) thresholding were applied according to BARCIST 1.0 criteria, comprising an individualized lower standardized uptake value (SUV) threshold and a Hounsfield unit range (-190;-10) [3]. In addition to assessing [^{18}F]fluorodeoxyglucose ([^{18}F]FDG) uptake in classical BAT depots (i.e. cervical and supraclavicular regions), [^{18}F]FDG uptake was evaluated in the upper mediastinal, axillary and paravertebral adipose tissue depots ('total body BAT'). Lastly, [^{18}F]FDG uptake was investigated in reference tissues (liver, cerebellum and descending aorta) as well as various muscles; m. sternocleidomastoideus, m. longus colli, m. trapezius, m. deltoideus, m. pectoralis major, m. psoas major and m. gluteus maximus.

Skin temperature analysis

Supraclavicular skin temperature was measured on the right supraclavicular fossa. Skin temperature at the right axilla was used as a proxy for core body temperature. Proximal skin temperature was calculated by the formula of Schellen et al. [4], as the average of the skin temperature at the scapula, lumbar zone, chest area and abdomen. Distal skin temperature was determined as the average temperature of the right hand and left foot.

Magnetic resonance imaging data acquisition and analysis

Participants were placed in a head-first supine position in the MRI scanner, with their head in a 16-channel head and neck coil, while a 16-channel anterior array was placed on their torso. A three-dimensional six-point chemical-shift encoded gradient-echo acquisition was applied with the following parameters: repetition time TR=16.5 ms, first echo time TE=1.79 ms, echo time separation ΔTE=1.98 ms, flip angle=3°, field-of-view of 480 mm × 300 mm × 90 mm (Right-Left, Foot-Head, Anterior-Posterior), 1.1 mm isotropic resolution, 4 retrospectively averaged signal averages.

An in-house water-fat separation algorithm based on the estimation of main magnetic field inhomogeneity was used for magnetic resonance imaging (MRI) characterization of the supraclavicular adipose tissue depot. The algorithm comprises a-priori knowledge regarding the multi-peak fat spectrum and assumes mono-exponential effective transverse relaxation time T2*. Initially, a low-resolution reconstruction was performed by using an estimate for the main magnetic field inhomogeneity. Subsequently, a region growing scheme was used to extrapolate the solution from correctly reconstructed parts in order to acquire the reconstructed water and fat images at high resolution [5-8]. Fat fraction maps were reconstructed according to formula [1], where x, y and z denote

$$Signal\ fat\ fraction(x,y,z) = \frac{Fat(x,y,z)}{Water(x,y,z)+Fat(x,y,z)} \quad [1]$$

the coordinates of a voxel in the directions: Right-Left, Foot-Head, Anterior-Posterior, respectively. Lipid content of the supraclavicular adipose depot was calculated as the product of the average fat fraction and volume.

Regions of interest encompassing the established location of the unilateral left supraclavicular adipose tissue depot were manually drawn on the baseline scans by A.S.M. and K.F.M.B. Registration was performed using the open-source image registration toolbox Elastix [9, 10]. The first echoes of the pre- and post-intervention image stacks were co-registered by first aligning them in an affine manner. Afterwards, deformable registration was performed with a three-dimensional B-spline transform with a 10×10×10 mm3 grid. To calculate the deformation field, we used adaptive stochastic gradient descent with two resolutions for optimization and Mattes mutual information as the similarity measure. The parameter file that was used for performing the registration can be downloaded from http://elastix.bigr.nl/wiki/index.php/Par0048. Finally, the calculated deformation field from the registration was used to transform the baseline regions of interest to the post-intervention image coordinates for the assessment of estimated BAT volume and fat fraction. A fat fraction threshold range of 0.5–1.0 was used for data analysis.

REFERENCES

1. Bakker LE, Boon MR, van der Linden RA, Arias-Bouda LP, van Klinken JB, Smit F, et al. Brown adipose tissue volume in healthy lean south Asian adults compared with white Caucasians: a prospective, case-controlled observational study. Lancet Diabetes Endocrinol. 2014;2:210-7.
2. Boellaard R, Delgado-Bolton R, Oyen WJ, Giammarile F, Tatsch K, Eschner W, et al. FDG PET/CT: EANM procedure guidelines for tumour imaging: version 2.0. Eur J Nucl Med Mol Imaging. 2015;42:328-54.
3. Chen KY, Cypess AM, Laughlin MR, Haft CR, Hu HH, Bredella MA, et al. Brown Adipose Reporting Criteria in Imaging STudies (BARCIST 1.0): Recommendations for Standardized FDG-PET/CT Experiments in Humans. Cell Metab. 2016;24:210-22.
4. Schellen L, Loomans MG, de Wit MH, Olesen BW, van Marken Lichtenbelt WD. The influence of local effects on thermal sensation under non-uniform environmental conditions--gender differences in thermophysiology, thermal comfort and productivity during convective and radiant cooling. Physiol Behav. 2012;107:252-61.
5. Reeder SB, Pineda AR, Wen Z, Shimakawa A, Yu H, Brittain JH, et al. Iterative decomposition of water and fat with echo asymmetry and least-squares estimation (IDEAL): application with fast spin-echo imaging. Magn Reson Med. 2005;54:636-44.
6. Reeder SB, Wen Z, Yu H, Pineda AR, Gold GE, Markl M, et al. Multicoil Dixon chemical species separation with an iterative least-squares estimation method. Magn Reson Med. 2004;51:35-45.
7. Yu H, McKenzie CA, Shimakawa A, Vu AT, Brau AC, Beatty PJ, et al. Multiecho reconstruction for simultaneous water-fat decomposition and T2* estimation. J Magn Reson Imaging. 2007;26:1153-61.
8. Yu H, Reeder SB, Shimakawa A, Brittain JH, Pelc NJ. Field map estimation with a region growing scheme for iterative 3-point water-fat decomposition. Magn Reson Med. 2005;54:1032-9.
9. Klein S, Staring M, Murphy K, Viergever MA, Pluim JP. elastix: a toolbox for intensity-based medical image registration. IEEE Trans Med Imaging. 2010;29:196-205.
10. Shamonin DP, Bron EE, Lelieveldt BP, Smits M, Klein S, Staring M, et al. Fast parallel image registration on CPU and GPU for diagnostic classification of Alzheimer's disease. Front Neuroinform. 2013;7:50.

Tables

Supplementary Table 1 Effect of exenatide on body weight and composition.

	All participants (N=24)		Europids (N=12)		South Asians (N=12)		
	Pre	**Post**	**Pre**	**Post**	**Pre**	**Post**	p-value for interaction
SBP (mmHg)	120±2	116±2 **	123±2	119±3 *	116±2 †	113±2 *†	0.879
DBP (mmHg)	78±2	76±1	81±3	78±2	75±2 †	75±1	0.319
Heart rate (bpm)	61±2	67±2 ***	67±2	70±3 *	55±3 ††	64±2 $^{***\sim}$	0.010

Pre=before exenatide, post=after exenatide. Data were analysed by a two factor mixed design ANOVA and are presented as mean±SEM. P-value for interaction is exenatide treatment*ethnicity. ˜p<0.1, *p<0.05, **p<0.01 post *vs* pre exenatide. †p<0.05, ††p<0.01 South Asians *vs* Europids.

Supplementary Table 2 Effect of exenatide on blood pressure and heart rate.

	All participants (N=24)		Europids (N=12)		South Asians (N=12)		
	Pre	**Post**	**Pre**	**Post**	**Pre**	**Post**	p-value for interaction
SBP (mmHg)	120±2	116±2 **	123±2	119±3 *	116±2 †	113±2 *†	0.879
DBP (mmHg)	78±2	76±1	81±3	78±2	75±2 †	75±1	0.319
Heart rate (bpm)	61±2	67±2 ***	67±2	70±3 *	55±3 ††	64±2 $^{***\sim}$	0.010

Pre=before exenatide, post=after exenatide. Data were analysed by a two factor mixed design ANOVA and are presented as mean±SEM. P-value for interaction is exenatide treatment*ethnicity. *p<0.05, **p<0.01, ***p<0.001 post vs pre exenatide. ˜p<0.1, †p<0.05, ††p<0.01 South Asians vs Europids. DBP=diastolic blood pressure, SBP=systolic blood pressure.

Supplementary Table 3 Effect of exenatide on [18F]FDG uptake by brown adipose tissue

	All participants (N=23)		Europids (N=12)		South Asians (N=11)		
	Pre	**Post**	**Pre**	**Post**	**Pre**	**Post**	p-value for interaction
Classical BAT depots							
BAT metabolic volume (mL)	79±14	101±13 *	63±18	84±19	97±22	119±16	0.933
SUV_{mean}	2.7±0.2	3.0±0.2 *	2.3±0.2	2.7±0.2	3.0±0.4	3.4±0.4	0.862
SUV_{peak}	8.1±1.5	9.5±1.2	6.0±1.3	7.6±1.5	10.4±2.7	11.6±1.9	0.865
Metabolic BAT activity (g)	277±67	350±58	186±63	268±76	375±117	439±84	0.842
Total body BAT depots							
BAT metabolic volume (mL)	123±21	154±19 *	100±27	132±30	147±32	178±24	0.974
SUV_{mean}	2.5±0.2	2.8±0.2 ˜	2.2±0.2	2.5±0.2	2.8±0.3	3.1±0.3	0.895
SUV_{peak}	8.2±1.5	9.5±1.2	6.1±1.2	7.6±1.5	10.4±2.7	11.6±1.9	0.888
Metabolic BAT activity (g)	382±87	486±78 ˜	270±86	390±107	503±151	591±111	0.788

Classical brown adipose tissue (BAT) is defined as the bilateral cervical and supraclavicular BAT depots. Total body BAT is defined as the bilateral cervical, supraclavicular, upper mediastinal, axillary and paravertebral BAT depots. One of the 12 South Asian participants was excluded due to movement of the participant during a scan. Pre=before exenatide, post=after exenatide. Data were analysed by a two factor mixed design ANOVA and are presented as mean±SEM. P-value for interaction is exenatide treatment*ethnicity. ˜p<0.1, *p<0.05 post vs pre exenatide.

Supplementary Table 4 Effect of exenatide on [18F]FDG uptake by reference tisues, skeletal muscle and white adipose tissue

SUVmean	All participants (N=23)		Europids (N=12)		South Asians (N=11)		p-value for interaction
	Pre	Post	Pre	Post	Pre	Post	
Reference tissues							
Liver	2.12±0.07	2.08±0.06	2.06±0.07	1.99±0.05	2.20±0.12	2.18±0.11	0.663
Cerebellum	7.47±0.34	7.59±0.28	7.36±0.37	7.34±0.35	7.60±0.60	7.86±0.45	0.583
Aorta descendens	1.39±0.06	1.34±0.04	1.35±0.07	1.23±0.04	1.44±0.08	1.45±0.06 †	0.249
Skeletal muscle							
M. Sternocleidomastoideus	1.03±0.08	1.02±0.10	0.93±0.10	1.00±0.14	1.13±0.12	1.06±0.12	0.555
M. Longus colli	1.55±0.18	1.78±0.31	1.16±0.21	1.58±0.25	1.94±0.25	1.99±0.58	0.527
M. Trapezius	0.55±0.03	0.47±0.03 *	0.52±0.05	0.50±0.03	0.58±0.05	0.44±0.04 **	0.040
M. Deltoideus	0.56±0.04	0.54±0.04	0.58±0.08	0.57±0.08	0.54±0.03	0.50±0.03	0.557
M. Pectoralis major	0.51±0.03	0.59±0.03 *	0.50±0.04	0.63±0.05 *	0.52±0.06	0.55±0.04	0.141
M. Psoas major	0.78±0.07	0.99±0.07 ***	0.84±0.11	1.11±0.11 **	0.72±0.07	0.86±0.07 ˜	0.207
M. Gluteus maximus	0.45±0.02	0.46±0.02	0.44±0.03	0.46±0.03	0.45±0.02	0.46±0.04	0.926
White adipose tissue							
Subcutaneous, abdominal	0.29±0.03	0.30±0.03	0.30±0.03	0.30±0.06	0.27±0.05	0.30±0.04	0.778
Subcutaneous, dorsocervical	0.47±0.03	0.46±0.03	0.48±0.04	0.52±0.04	0.46±0.04	0.40±0.04 †	0.847
Visceral, paracolic	0.71±0.08	0.74±0.08	0.71±0.11	0.75±0.11	0.72±0.12	0.73±0.11	0.106

One of the 12 South Asian participants was excluded from all [18F]FDG-PET/CT analyses due to movement of the participant. Pre=before exenatide, post=after exenatide. Data were analysed by a two factor mixed design ANOVA and are presented as mean±SEM. P-value for interaction is exenatide treatment*ethnicity. ˜p<0.1, *p<0.05, **p<0.01, ***p<0.001 post vs pre exenatide. ˜p<0.1, †p<0.05 South Asians vs Europids.

Supplementary Table 5: Effect of exenatide on the supraclavicular adipose tissue fat fraction and volume per ethnicity

	Europids (N=12)		**South Asians (N=12)**		p-value for interaction
	Pre	**Post**	**Pre**	**Post**	
Supraclavicular adipose tissue fat fraction	0.751±0.011	0.748±0.009	0.739±0.015	0.743±0.015	0.519
Supraclavicular adipose tissue volume (mL)	29.7±3.1	29.1±3.3	32.3±4.7	31.4±4.9	0.827

Fat fraction thresholds were set at 0.5-1.0. Pre=before exenatide, post=after exenatide. Data were analysed by a two factor mixed design ANOVA and are presented as mean±SEM. P-value for interaction is exenatide treatment*ethnicity.

Figures

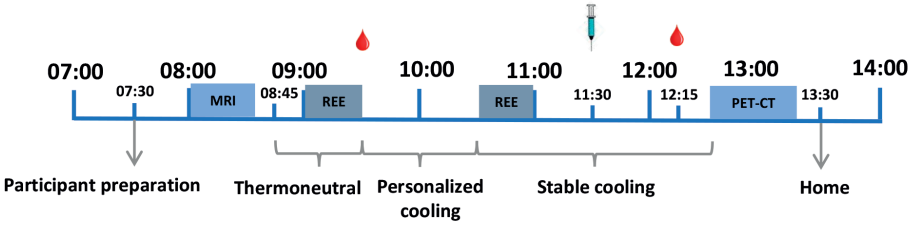

- Body impedance analysis
- Insert cannula
- 08:45-09:00 Attach iButtons
- 09:00-09:30: Indirect calorimetry
- 09:30: Blood draw
- 10:30-11:00: Indirect calorimetry
- 11:30: [^{18}F]FDG injection
- 12:15: Blood draw

Supplementary Fig. 1 Overview identical study day before and after the exenatide treatment period

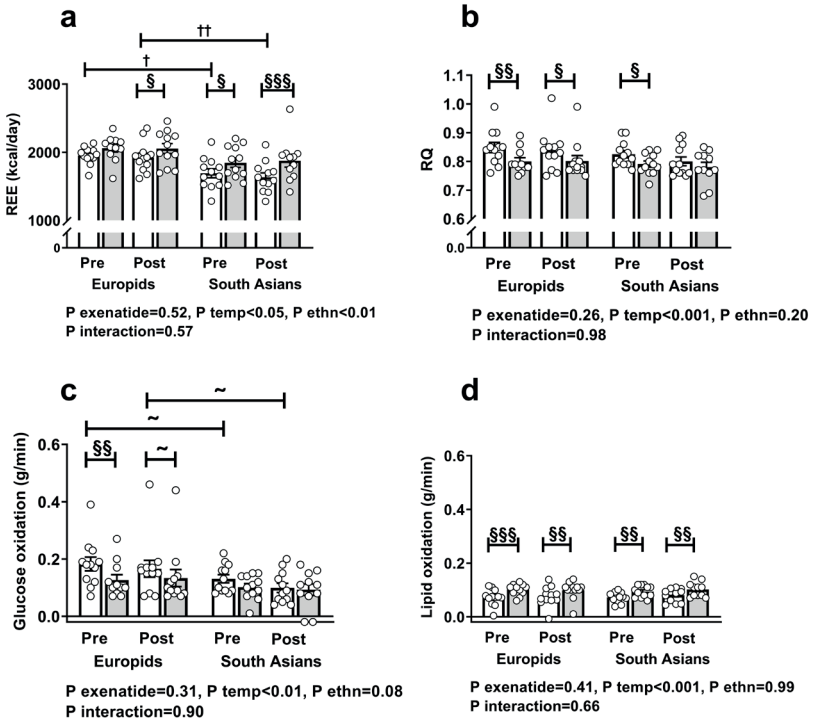

Supplementary Fig. 2 Exenatide does not affect energy metabolism in either ethnicity
The effect of exenatide on thermoneutral and cold-induced resting energy expenditure (REE) (**a**), respiratory quotient (RQ) (**b**), glucose oxidation (**c**) and lipid oxidation (**d**) per ethnicity (N=12 South Asians and N=12 Europids). Pre=before exenatide, post=after exenatide. White bars are thermoneutral, grey bars are during short term cooling. Data were analysed by linear mixed models and are presented as mean±SEM.. P-values for the main effect of exenatide treatment (exenatide), temperature (temp) and ethnicity (ethn) and their interaction (exenatide*temp*ethn) are shown below the figures. §p<0.05, §§p<0.01, §§§p<0.001 post-hoc p-values cold *vs* thermoneutrality. ˜p<0.1, †p<0.05, ††p<0.01 post-hoc p-values South Asians *vs* Europids.

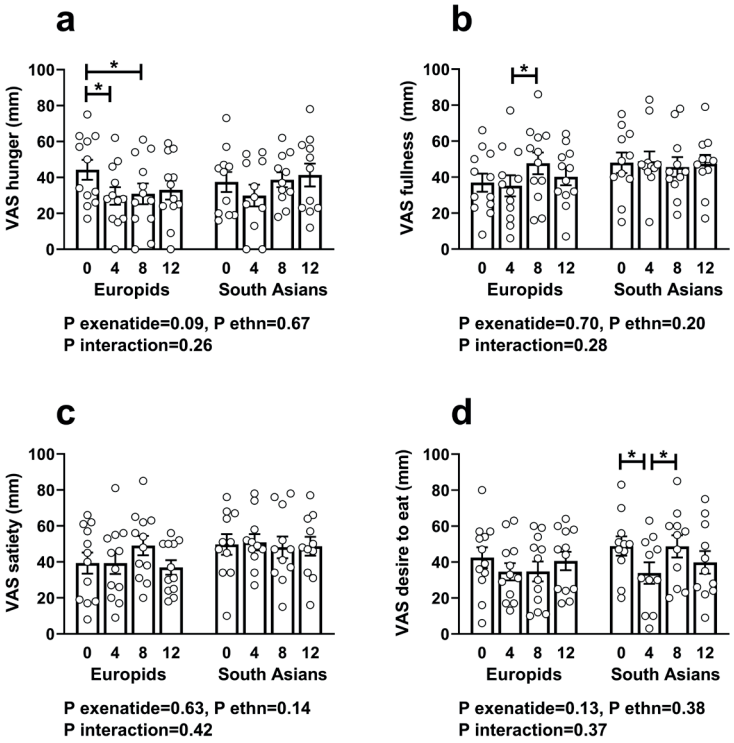

Supplementary Fig. 3 Exenatide reduces the feeling of hunger in Europids and desire to eat in South Asians during the first weeks of treatment

The effect of exenatide on subjective ratings for hunger (**a**), fullness (**b**), satiety (**c**) and desire to eat (**d**) measured every 4 weeks per ethnicity (N=11 South Asians and N=12 Europids). One of the 12 South Asian participants was excluded due to incomplete questionnaires. Higher values (mm) indicate higher ratings. Data were analysed by a two factor mixed design ANOVA and presented as mean±SEM. P-values for the main effect of exenatide treatment (exenatide), and ethnicity (ethn) and their interaction (exenatide*ethn) are shown below the figures. *p<0.05 post-hoc p-value effect of exenatide.

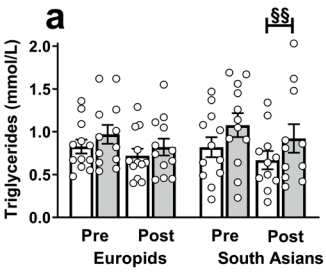

P exenatide=0.33, P temp=0.24, P ethn=0.71
P interaction=0.90

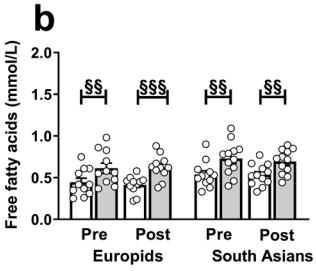

P exenatide=0.59, P temp<0.001, P ethn=0.12
P interaction=0.38

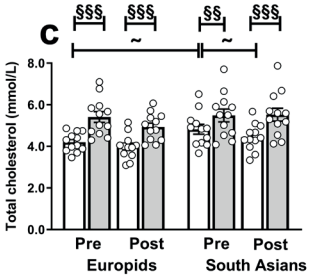

P exenatide<0.05, P temp<0.001, P ethn=0.11
P interaction=0.05

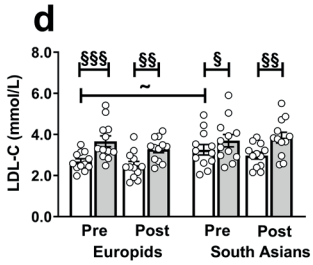

P exenatide=0.13, P temp<0.001, P ethn=0.13
P interaction=0.05

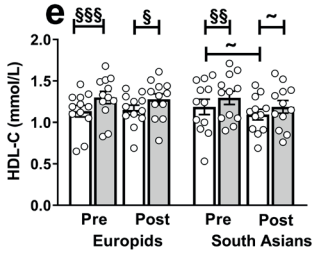

P exenatide=0.13, P temp<0.001, P ethn=0.80
P interaction=0.77

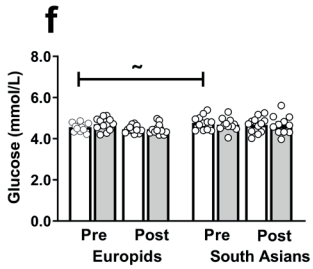

P exenatide=0.09, P temp=0.84, P ethn=0.10
P interaction=0.16

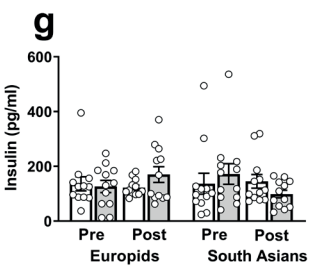

P exenatide=0.69, P temp=0.70, P ethn=0.98
P interaction<0.01

Supplementary Fig 4. Exenatide does not significantly affect lipid, glucose or insulin levels in either ethnicity The effect of exenatide on thermoneutral and cold-induced fasted serum triglycerides (**a**), free fatty acids (**b**), total cholesterol (**c**), LDL-cholesterol (LDL-C) (**d**)**,** HDL-cholesterol (HDL-C) (**e**), plasma glucose (**f**) and serum insulin (**g**) per ethnicity (N=12 South Asians and N=12 Europids). Pre=before exenatide, post=after exenatide. White bars are thermoneutral, grey bars are during short term cooling. Data were analysed by linear mixed models and are presented as mean±SEM. P-values for the main effect of exenatide treatment (exenatide), temperature (temp) and ethnicity (ethn) and their interaction (exenatide*temp*ethn) are shown below the figures. ˜p<0.1, §p<0.05, §§p<0.01, §§§p<0.001 post-hoc p-values cold *vs* thermoneutrality. ˜p<0.1 post-hoc p-values South Asians *vs* Europids.

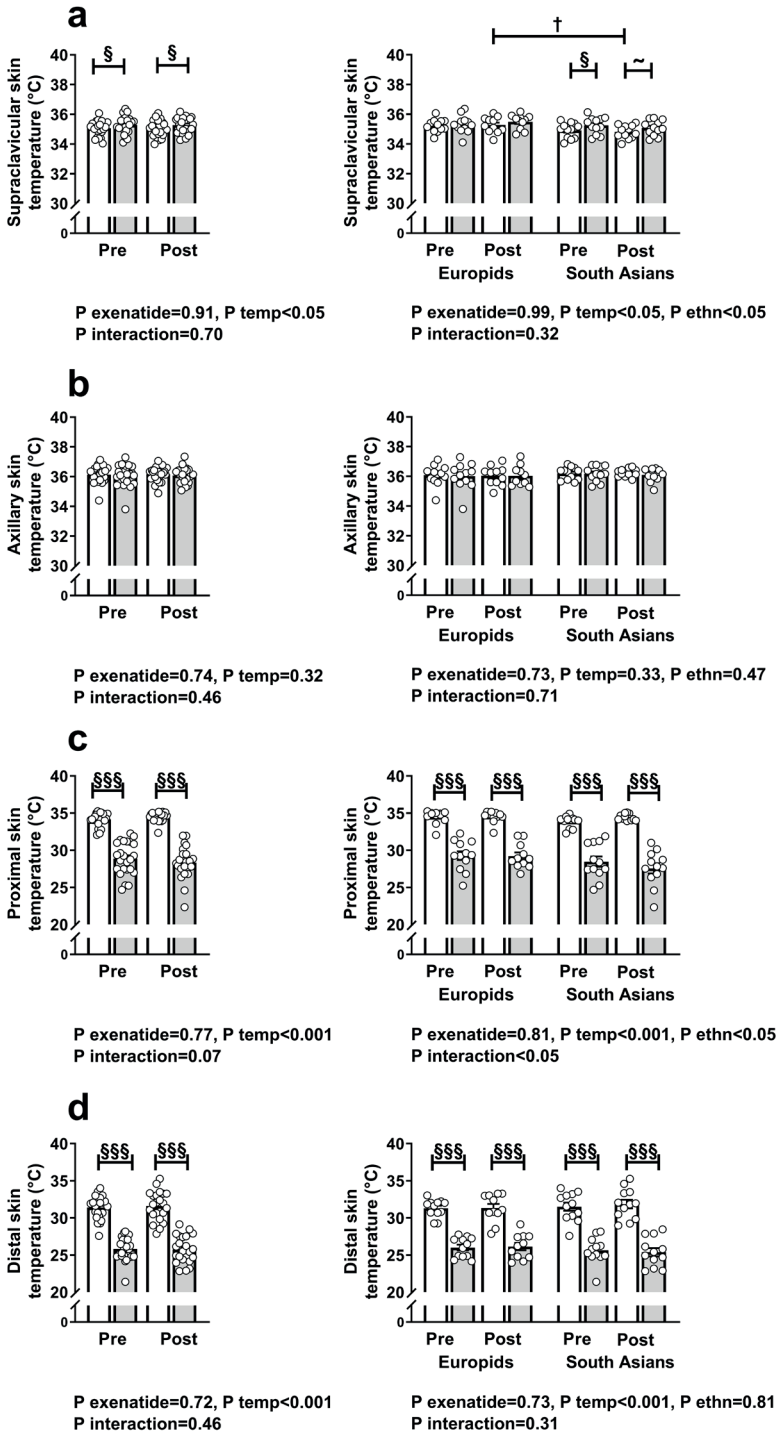
a
Supraclavicular skin temperature (°C)
§
§
†
§
~
Pre
Post
Europids
South Asians
P exenatide=0.91, P temp<0.05
P interaction=0.70
P exenatide=0.99, P temp<0.05, P ethn<0.05
P interaction=0.32
b
Axillary skin temperature (°C)
P exenatide=0.74, P temp=0.32
P interaction=0.46
P exenatide=0.73, P temp=0.33, P ethn=0.47
P interaction=0.71
c
Proximal skin temperature (°C)
§§§
P exenatide=0.77, P temp<0.001
P interaction=0.07
P exenatide=0.81, P temp<0.001, P ethn<0.05
P interaction<0.05
d
Distal skin temperature (°C)
P exenatide=0.72, P temp<0.001
P interaction=0.46
P exenatide=0.73, P temp<0.001, P ethn=0.81
P interaction=0.31

Supplementary Fig 5. Exenatide does not affect the supraclavicular, axillary, proximal or distal skin temperature in the total study population or in either ethnicity

The effect of exenatide on thermoneutral and cold-induced supraclavicular skin temperature (a), axillary skin temperature (b), proximal skin temperature (c) and distal skin temperature (d) in the total study cohort and per ethnicity (N=12 South Asians and N=12 Europids). Pre=before exenatide, post=after exenatide. White bars are thermoneutral, grey bars are during short term cooling. Data were analysed by linear mixed models and are presented as mean±SEM. For ethnicities combined, p-values for the main effect of exenatide treatment (treat) and temperature (temp) and their interaction (exenatide*temp) are shown below the figures. When taking ethnicity into account as a factor, p-values for the main effect of exenatide treatment (treat), temperature (temp) and ethnicity (ethn) and their interaction (exenatide*temp*ethn) are shown below the figures. ˜p<0.1, §p<0.05, §§§p<0.001 post-hoc p-values cold vs thermoneutrality. †p<0.05 post-hoc p-value South Asians vs